European Journal of Medicinal Chemistry 78 (2014) 294–303

Contents lists available at ScienceDirect

European Journal of Medicinal Chemistry

journal homepage: http://www.elsevier.com/locate/ejmech

Original article

Discovery of mixed type thymidine phosphorylase inhibitors endowed with antiangiogenic properties: Synthesis, pharmacological evaluation and molecular docking study of 2-thioxo-pyrazolo[1,5-*a*][1,3,5]triazin-4-ones. Part II

Hriday Bera [a,b,*], Probir kumar Ojha [c], Bee Jen Tan [b], Lingyi Sun [b], Anton V. Dolzhenko [b,d], Wai-Keung Chui [b,**], Gigi Ngar Chee Chiu [b]

[a] Gokaraju Rangaraju College of Pharmacy, Bachupally, Hyderabad 500090, India
[b] Department of Pharmacy, Faculty of Science, National University of Singapore, 18 Science Drive 4, Singapore 117543, Singapore
[c] Jadavpur University, Kolkata 700032, India
[d] School of Pharmacy, Monash University Sunway Campus, Jalan Lagoon Selatan, Bandar Sunway, Selangor, WA 46150, Malaysia

ARTICLE INFO

Article history:
Received 4 February 2014
Received in revised form
18 March 2014
Accepted 20 March 2014
Available online 21 March 2014

Keywords:
Pyrazolo[1,5-*a*][1,3,5]triazine
Thymidine phosphorylase inhibitors
Mixed-type inhibition
Breast cancer
Antiangiogenesis

ABSTRACT

In our drug discovery program, a series of 2-thioxo-pyrazolo[1,5-*a*][1,3,5]triazin-4-ones were designed, synthesized and evaluated for their TP inhibitory potential. All the synthesized analogues conferred a varying degree of TP inhibitory activity, comparable or better than positive control, 7-deazaxanthine (**7-DX**, **2**) (IC_{50} value = 42.63 μM). A systematic approach to the lead optimization identified compounds **3c** and **4a** as the most promising TP inhibitors, exhibiting mixed mode of enzyme inhibition. Moreover, selected compounds demonstrated the ability to attenuate the expression of the angiogenic markers (*viz.* MMP-9 and VEGF) in MDA-MB-231 cells at sublethal concentrations. In addition, molecular docking studies revealed the plausible binding orientation of these inhibitors towards TP, which was in accordance with the experimental results. Taken as a whole, these compounds would constitute a new direction for the design of novel TP inhibitors with promising antiangiogenic properties.

1. Introduction

Carcinoma is the leading cause of premature death in the world [1]. Due to the rapid advancement in cancer diagnosis and therapy, the life expectancy and survival rate of cancer patients have shown improvement, however, the overall clinical outcome of cancer is still unsatisfactory due to its high invasive and metastatic properties. In order to achieve therapeutic success in cancer patients, there is still room to develop new treatment strategies that target at various stages of *tumour* progression. A flurry of scientific investigations has identified angiogenesis as one of the important processes in cancer development. Angiogenesis was found to promote tumour growth and metastasis [2–4]. Moreover, in 1971, Folkman postulated that antiangiogenesis might be an effective *cancer treatment strategy* [5]. Since then, there was an increasing interest in exploring novel antiangiogenic agents for cancer therapy [6–9].

Among several angiogenic activators, thymidine phosphorylase (TP, EC 2.4.2.4) has been recognized as an important angiogenic protein that is frequently overexpressed within solid tumours [10]. In recent years, emerging data provided convincing evidence that TP and its metabolic product, 2-deoxy-D-ribose (2DDR) stimulate the secretion and/or expression of many angiogenic factors, such as MMPs and VEGF, which trigger a signalling cascade to induce endothelial cell migration, proliferation, elongation and sprouting. These events eventually lead to angiogenesis and cancer metastasis [11]. Therefore, TP has been implicated as a potential target for the development of chemotherapeutic agents [12,13]. An increasing number of studies in this field have discovered several potent TP inhibitors. Structurally, most of them are pyrimidin-2,4-dione derivatives. To date, only a few TP inhibitors incorporating heterobicyclic templates have been designed and reported [14–17]. Among them, **TPI** and **7-DX** (Fig. 1) have emerged as leading TP

* Corresponding author. Gokaraju Rangaraju College of Pharmacy, Bachupally, Hyderabad 500090, India.
** Corresponding author.
E-mail addresses: hriday.bera1@gmail.com (H. Bera), phacwk@nus.edu.sg (W.-K. Chui).

http://dx.doi.org/10.1016/j.ejmech.2014.03.063
0223-5234/

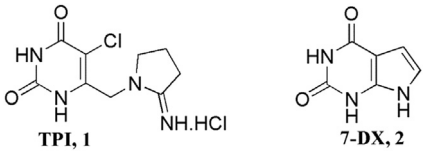

Fig. 1. Chemical structures of known TP inhibitors.

inhibitor candidates [18,19]. Although several potent inhibitors were generated and tested, very few TP inhibitors have progressed beyond the preclinical stage [20]. Therefore, the development of TP inhibitors possessing antiangiogenic activity is assumed to improve TP-targeted therapy.

The close structural similarity between pyrazolo[1,5-*a*][1,3,5] triazine and purine nuclei vindicated the development of pyrazolo [1,5-*a*][1,3,5]triazines as medicinally active compounds that would target several enzymes involved in the metabolism of biogenic purines and G-protein coupled purinergic signalling receptors [21]. A wide variety of attractive pharmacological effects of this scaffold has led us to investigate the anti-TP effects of pyrazolo[1,5-*a*][1,3,5] triazin-2,4-diones and their thioxo analogues which are bio-isosterically modified derivatives of **7-DX**. In this context, a small library of compounds bearing substituents at position C7 or C8 of the core ring structure was synthesized. Among various compounds synthesized, 2-thioxo analogues of pyrazolo[1,5-*a*][1,3,5] triazin-2,4-diones displayed various extent of TP inhibitory activity [16].

The success of the project inspired us to design molecules modified at both C7 and C8 positions of the fused ring structure for further biological evaluation. To study the effects of various substituents on the TP inhibitory activity, Craig plot directed approach [22] was employed. In the present study, a series of pyrazolo[1,5-*a*] [1,3,5]triazin-2-thioxo-4-one derivatives (Fig. 2) with differently substituted aromatic rings were synthesized. The synthesized compounds were subsequently evaluated for their *in vitro* TP inhibitory potential. To elucidate the mechanism of enzyme inhibition, a brief kinetic study was attempted. Moreover, selected compounds were exploited to investigate their antiangiogenic properties by performing experiments that demonstrate an inhibition of MMP-9 and VEGF expression in MDA-MB-231 cells. We also performed *in silico* molecular docking studies to explore the ligand binding site and possible interactions mode of the synthesized compounds with TP.

2. Results and discussion

2.1. Chemistry

The synthesis of the title compounds (**3**, **4**) was achieved *via* annulation of 1,3,5-triazine ring onto aminopyrazoles, as outlined in Schemes 1 and 2. The adopted synthetic procedures were based on previously disclosed methods [16,23–25]. The reaction of aminopyrazoles (**7** and **11**) with ethoxycarbonyl isothiocyanate in DMF

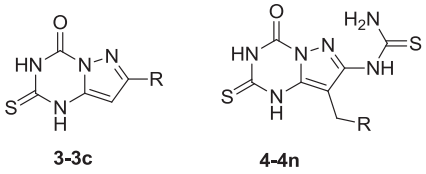

Fig. 2. Chemical structures of target compounds.

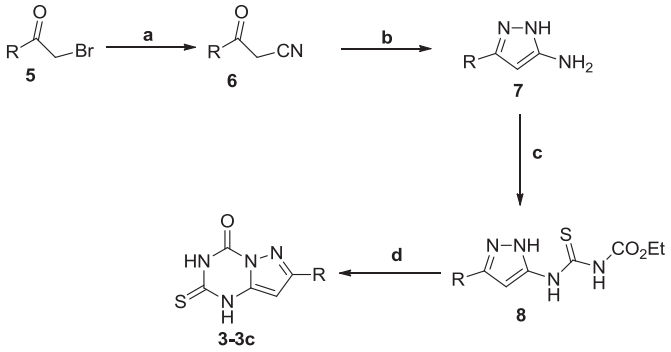

Scheme 1. Synthesis of target compounds (**3**–**3c**). Reagents and conditions: (a) NaCN, HCl, aqueous-ethanol, r.t. (b) $NH_2NH_2.H_2O$, methanol, MW, 140 °C, 1 h (c) $EtO_2CN{=}O$, DMF, r.t., 5 h (d) NaOH, 80% ethanol (aq.), 100 °C, 20 min.

afforded the thiourea derivatives (**8** and **12**) which underwent intramolecular heterocyclization in the presence of base, resulting in the formation of target compounds (**3**–**3c** and **4**–**4n** respectively).

Our synthetic strategy also employed two efficient and expeditious protocols to produce two key intermediates *viz.*, 5-aminopyrazoles (**7**) and 3,5-diaminopyrazoles (**11**). The reactions of commercially available substituted bromoacetophenones (**5**) with sodium cyanide gave cyanoacetophenones (**6**), which underwent a cyclocondensation reaction upon treatment with hydrazine hydrate under microwave irradiation to furnish **7** (Scheme 1) [26,27]. On the other hand, the preparation of 3,5-diaminopyrazoles (**11**) comprised the synthesis of mono-substituted malononitriles (**10**) *via* reductive alkylation of malononitrile with benzaldehydes (**9**) [28]. Subsequently, the reactions of intermediates (**10**) with hydrazine hydrate in refluxing ethanol yielded corresponding 3,5-diaminopyrazoles (**11**) (Scheme 2).

All the synthesized compounds (**3**–**3c** and **4**–**4n**) were characterized by melting points and various spectroscopic techniques (^{1}H NMR, ^{13}C NMR and MS). The purity of the compounds was assessed using reverse phase HPLC method and elemental analysis. Interestingly, the structures of compounds **3**, **4** were readily confirmed by ^{13}C NMR spectroscopy. The analysis of the ^{13}C NMR spectral data of compound **3** revealed that two sharp signals of carbonyl (C=O) and thiocarbonyl (C=S) carbon appeared at around 155.9 and 173.6 ppm respectively. Similarly, the characteristic signals of one carbonyl (C=O) and two thiocarbonyl (C=S)

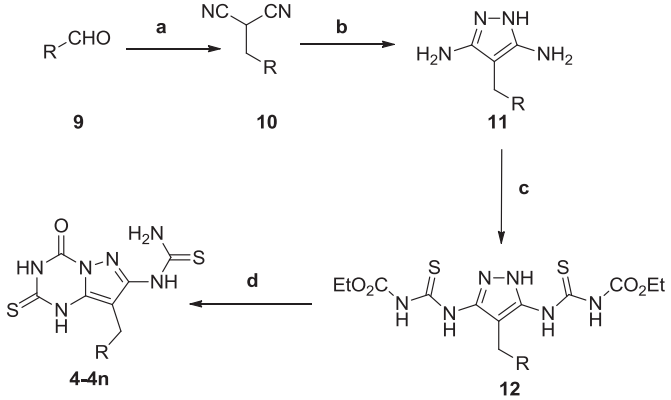

Scheme 2. Synthesis of target compounds (**4**–**4n**). Reagents and conditions: (a) mandalonitrile, aqueous-ethanol, $NaHB_4$, 1.0 M HCl, r.t. (b) $NH_2NH_2.H_2O$, Ethanol, reflux, 5–8 h (c) Ethoxycarbonyl isothiocyanate, DMF, r.t., 5 h (d) NaOH, 80% ethanol (aq.), 100 °C, 20 min.

carbon of compound **4** appeared around 151.9, 173.5 and 179.8 ppm respectively in ^{13}C NMR spectra. The purity of all compounds was satisfactory (above 95%).

2.2. Evaluation of biological activities

2.2.1. Anti-thymidine phosphorylase (Anti-TP) activity

Nineteen compounds (**3**, **4**) were tested for their TP inhibitory activity by a spectrophotometric coupled enzyme assay that used recombinant human thymidine phosphorylase, expressed in *E. coli* (T2807 − Sigma Aldrich) as the enzyme and thymidine as the substrate. The adopted protocol is a modification to the original method developed by Krenitsky (Krenitsky et al., 1979) [29]. The inhibitory potencies of compounds were expressed in terms of IC_{50} values and were compared with the reference inhibitor, **7-DX** (IC_{50} = 42.63 μM) (Table 1). The preliminary enzyme inhibition study of compounds (**3**–**3c**) suggested following structure–activity relationships: (1) Replacement of the phenyl ring of compound **3** (IC_{50} = 46.21 μM) by a bulky *t-butyl* group at C7 resulted in significant reduction in affinity for TP, as evident in compound **3a** (IC_{50} = 55.70 μM). This result indicated that the *t-butyl* group might present a negative steric hindrance effect to the binding site of the enzyme. (2) Introduction of a substituent (CN) into the structure of compound **3** demonstrated substantial improvement in binding interactions, as observed in compound **3b** (IC_{50} = 30.32 μM). (3) Moreover, disubstituted analogue **3c** (IC_{50} = 9.07 μM) exhibited significantly enhanced inhibition profile relative to mono substituted compound **3b**.

Based on the preliminary enzyme inhibition results, we were prompted to modify both C7 and C8 positions of the fused ring structure using similar synthetic protocol. The resulting disubstituted compound **4** (IC_{50} = 29.92 μM) was found to be more favourable for TP inhibitory activity than the mono substituted analogue **3**. With the aim of enhancing the inhibition properties of compound **4**, a number of substituents scattered around all the four quadrants of Criag plot were selected in this study and they were introduced at the *para* position of the phenyl ring of compound **4.** This approach generated a variety of analogues of **4** which exhibited significantly different levels of TP inhibitory activity, with IC_{50} values ranging from 4.0 to 52.0 μM (Table 1).

In series **4**, with few exceptions (**4g**, **4h** and **4i**), substituted compounds, no matter having electron-withdrawing or electron-donating groups, conferred a significantly higher activity than the parent compound **4** (Table 1). Compound **4e** (IC_{50} = 19.98 μM), carrying a methyl moiety (+π, −σ), showed almost a 2.6-fold increase in inhibitory activity as compared to **4g** (IC_{50} = 51.44 μM) that had a methoxy substituent (−π, −σ). In addition, compound **4f** (IC_{50} value = 12.56 μM), bearing an ethyl group, displayed more effective inhibition than compound **4e** having a methyl substituent. Moreover, among all the compounds evaluated, compound **4a** bearing a CF_3 moiety was observed to have the best anti-TP activity and it exhibited 12.8, 7.8 and 11.2-fold enhancement in inhibitory activity as compared to compounds **3**, **4** and **7-DX** respectively. The highest TP inhibitory activity of compound **4a** was possibly due to its high lipophilicity, imparted by introduction of a CF_3 group. Overall, the lipophilicity of compounds was considered to be an important prerequisite to elicit a prominent TP inhibitory effect.

These findings inspired us to modify compound **4** by inserting various hydrophobic motifs *viz*., biphenyl, phenoxyphenyl and naphthalene groups at the C8 position. Interestingly, compounds **4j**, **4k** and **4l** demonstrated an improved inhibition profile towards TP relative to compound **4**. Our investigation was further extended by introducing 2-furyl and 2-thienyl moieties at the C8 position of the core scaffold in order to explore the influence of different aromatic heterocycles in activity. However, such effort did not reveal any significant improvement in potency, as evident in compounds **4m** and **4n**.

Table 1
Thymidine phosphorylase inhibitory activity of the synthesized compounds (**3**, **4**).

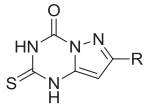

3-3c

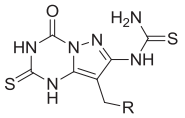

4-4n

Entry	Cpd	*R*	TP inhibition activity[a,b] IC_{50} (μM)
1	**3**	Ph	46.21 ± 1.82
2	**3a**	$C(Me)_3$	55.70 ± 5.13
3	**3b**	4-CNC_6H_4–	30.32 ± 2.74
4	**3c**	3,4-$Cl_2C_6H_3$–	9.07 ± 1.23
5	**4**	Ph	29.92 ± 4.39
6	**4a**	4-$CF_3C_6H_4$-	3.82 ± 0.78
7	**4b**	4-ClC_6H_4-	10.54 ± 2.50
8	**4c**	4-BrC_6H_4-	14.78 ± 1.86
9	**4d**	4-FC_6H_4-	22.65 ± 4.65
10	**4e**	4-MeC_6H_4-	19.98 ± 4.26
11	**4f**	4-EtC_6H_4-	12.56 ± 1.53
12	**4g**	4-$MeOC_6H_4$-	51.44 ± 3.95
13	**4h**	4-OHC_6H_4-	37.38 ± 4.93
14	**4i**	4-CNC_6H_4-	51.53 ± 2.69
15	**4j**	4-PhC_6H_4-	6.11 ± 0.83
16	**4k**	4-$OPhC_6H_4$-	4.46 ± 0.42
17	**4l**	1-naphthyl	4.29 ± 0.88
18	**4m**	2-furyl	36.72 ± 5.65
19	**4n**	2-thienyl	27.69 ± 4.02
20	**7-Dx**		42.63 ± 5.25

[a] Values are means of three experiments.
[b] Values are presented as means ± SD.

2.2.2. Mechanism of enzyme inhibition

In an attempt to explore the mode of enzyme inhibition, a brief enzyme inhibition kinetic study was performed. Compounds **3c** and **4a**, endowed with promising TP inhibitory activity were selected for kinetic analysis. In this study, compounds **3c** and **4a** were found to exhibit mixed- type inhibition with respect to thymidine as the variable substrate, since the reciprocal plots for compounds showed straight lines that intersected each other in the left panel (Fig. 3). This was further confirmed by the fact that increased inhibitor concentration was accompanied by an increase in the K_m values and a decrease in the V_{max} values.

The model of Scheme 3 was adopted to explain the mixed-type inhibition. Compounds **3c** and **4a** were assumed to interact with the enzyme (E) as well as enzyme-substrate (ES) complex without affecting substrate binding [30]. We also calculated the values of inhibition constants (K_i and αK_i) by replotting the slopes and intercepts of the double reciprocal plots against the inhibitor concentrations (Table 2). The data clearly indicated that the inhibitors had stronger affinity for the free enzyme than enzyme-substrate complex ($\alpha > 1$). Moreover, the enzyme–inhibitor complex exhibited reduced affinity for substrate in comparison to free enzyme ($\alpha > 1$) (Scheme 3). Due to structural variability in the core scaffold, compounds **3c** and **4a** showed different modes of interaction as compared to **7-DX**, which behaved as a competitive or mixed-type inhibitor of the enzyme in the presence of variable thymine concentrations [31].

2.2.3. Antiangiogenic activity: inhibition of MMP-9 and VEGF expression

Matrix metallopeptidase 9 (MMP-9) belongs to a family of zinc-*dependent endopeptidases*. It plays a pivotal role in the accelerated

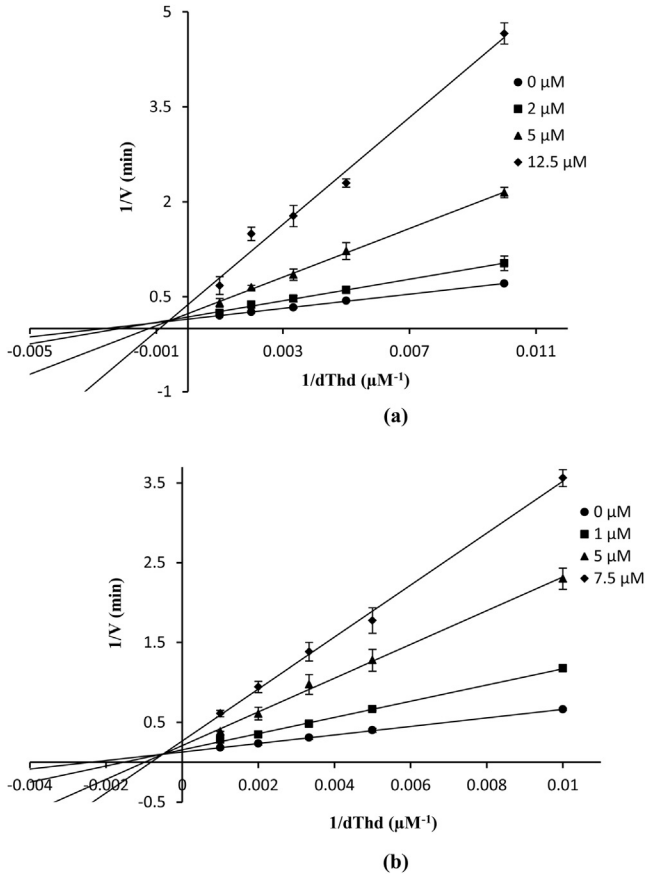

Fig. 3. Lineweaver–Burk plots of TP inhibition by **3c** (A) and **4a** (B), in the presence of variable concentrations of dThd, demonstrating mixed type enzyme inhibition. Results are presented as means ± SD; SD denoted by error bars (Experiments carried out in triplicate).

breakdown of extracellular matrix surrounding the tumour cells that eventually results in increased tumour cell migration, invasion and metastasis [32]. On the other hand, vascular endothelial growth factor (VEGF) plays a paradoxical role in tumour angiogenesis by inducing the proliferation, migration and survival of endothelial cells [33]. A large number of studies reported that TP is associated with the induction of MMP-9 and VEGF expression in tumour cells [10]. Moreover, a significant correlation was observed between VEGF and TP expression in solid tumours, as both proangiogenic factors share the same transcription site [34]. Compounds (**3c**, **4a**, **4j**, **4k** and **4l**) that showed attractive *in vitro* TP inhibition profile (IC_{50} less than 10 μM), were examined for their ability to suppress MMP-9 and VEGF production in MDA-MB-231 cells.

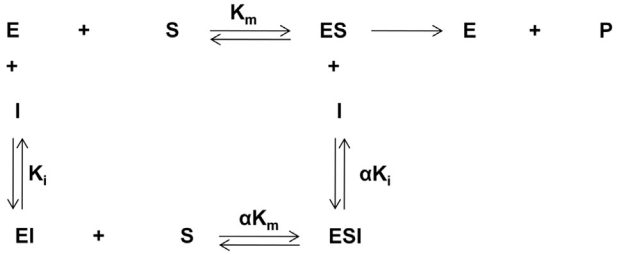

Scheme 3. Enzyme kinetic model explaining mixed type inhibition.

Table 2
A summary of the kinetic parameters of **3c** and **4a**.

Cpd	Substrate	K_i value (μM)[a,b]	α	Type of inhibition
3c	dThd	1.77 ± 0.35	4.10	Mixed type
4a	dThd	1.65 ± 0.10	5.20	Mixed type

[a] Values are means of three experiments.
[b] Values are presented as means ± SD.

To explore the inhibitory effects of the selected compounds on PMA-induced MMP-9 expression, gelatine zymography [35] was conducted. In this study, MDA-MB-231 cells *were treated* with the indicated concentrations of compounds (25–100 μM) and the proteolytic activity of MMP-9 (band corresponded to the MW of 92 kDa) was investigated. The results conferred that all compounds dose dependently attenuated MMP-9 expression (Fig. 4a). Quantitative densitometric analysis of the zymograms showed that all compounds (except **4a**) significantly inhibited MMP-9 expression at concentrations of 50 and 100 μM ($p < 0.05$) (Fig. 4b). Moreover, the inhibitory effects of these compounds on VEGF expression were investigated by enzyme-linked immunosorbent assay (ELISA) [15]. As depicted in Fig. 4c, the expression of VEGF was markedly reduced by all the tested compounds (**3c**, **4a**, **4j**, **4k** and **4l**) at doses ranging from 25 to 100 μM, as compared to vehicle control ($p < 0.05$). In contrast, the reference TP inhibitor (**7-DX**) did not exert any significant inhibitory effect on MMP-9 and VEGF expression even at very high concentration (100 μM) (Fig. 4–c). In order to ascertain the inhibitory effects of the compounds on MMP-9 and VEGF expression were not due to their cytotoxic effects, a cell viability assay [36] was conducted on MDA-MB-231 cells. An insignificant growth-inhibitory effect (cell viability 80–100%) was observed with all doses of **7-DX** and each compound tested (Fig. 4d).

It is noteworthy that the compounds (**4a**, **4j**, **4k** and **4l**) bearing substitutions at positions C7 and C8, displayed a higher inhibitory activity against MMP-9 and VEGF as compared to mono substituted analogue (**3c**). Most TP inhibitors discovered so far are substituted uracil analogues that compete with the substrate for access to the catalytic *cleft* of TP [11]. In contrast, compounds (**3**, **4**) represented a unique structural class of TP inhibitors and were assumed to interact to the enzyme at *distinct* sites, leading to attenuation of TP-induced upregulation of MMP-9 and VEGF. The kinetic behaviour of these compounds strongly supported our assumption.

2.3. Molecular docking study

To gain a deeper insight into the binding mode and to explore the detailed molecular interactions of the synthesized compounds, the geometry optimized structures of the inhibitors were docked into the binding sites of TP (PDB code: 2WK6) [37] using Discovery Studio 2.1 (Accelrys Inc, San Diego, CA, USA) [38]. Before docking, the docking protocol was validated by comparing the predicted binding orientation of bound ligand, 5-iodouracil (**5-IUR**) with the reported crystallographic interactions [37]. The observed binding modes of **5-IUR** in the crystal structure were strikingly well-aligned with the predicted docking poses (rmsd = 0.497Å) (Fig. S1, in Supplementary Information).

To illustrate the kinetic behaviour of the synthesized inhibitors, two binding pockets *viz.* site A (**5-IUR** binding site) and site B (allosteric site proximal to the **5-IUR** binding site) were identified and the docked conformations at two different sites were compared with respect to their docking scores. The site B is composed of several amino acid residues (Leu423, Val425, Asp426, Val427, Ala469, Arg279, Gly278, Pro472, Asp304, Ser471, Asp301, Pro300, Pro299, Ala468, Lys275 and Pro276) located in the vicinity

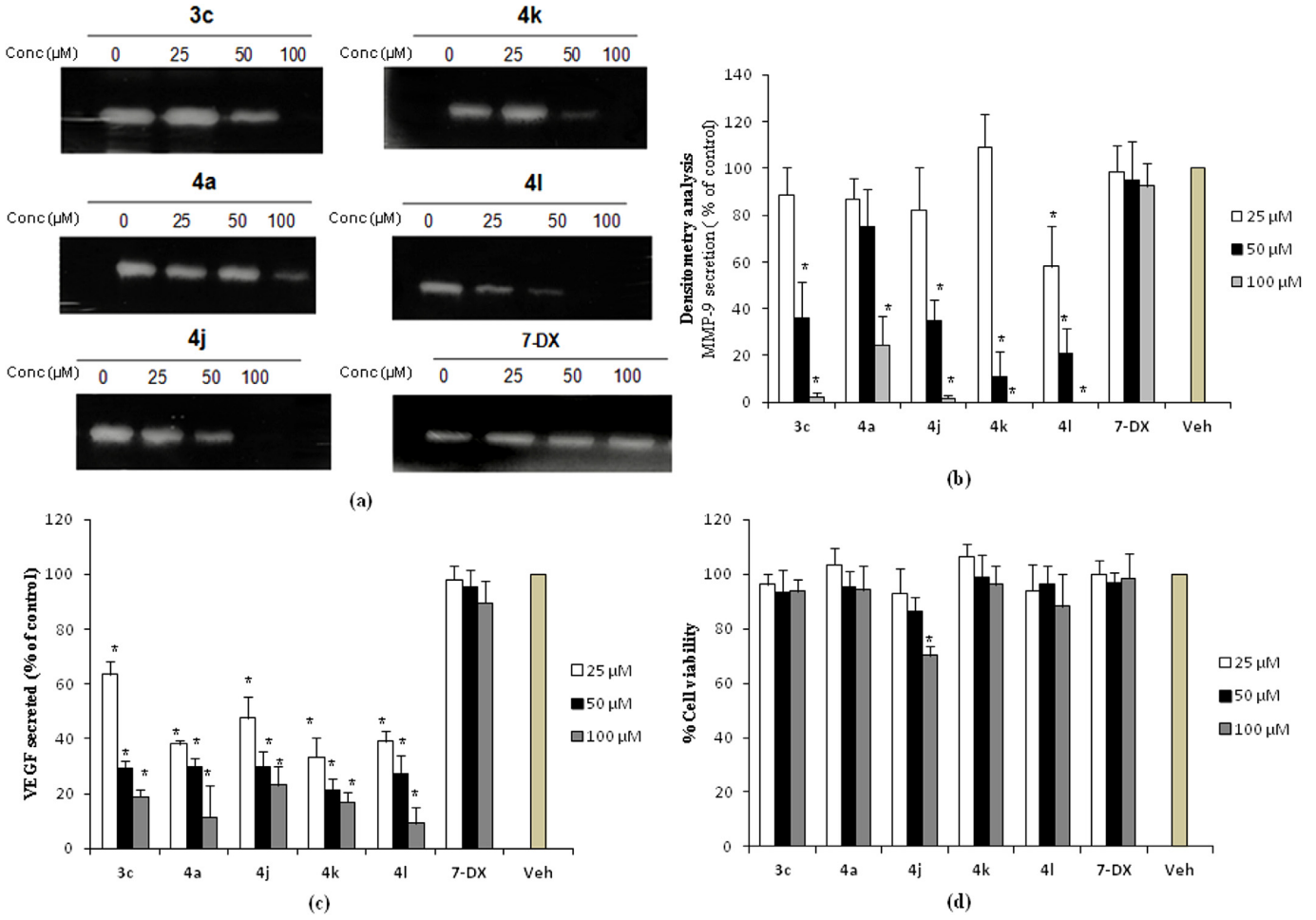

Fig. 4. Effect of selected compounds (**3c**, **4a**, **4j**, **4k** and **4l**) and **7-DX** on MMP-9 and VEGF expression and cell growth in MDA-MB-231 cells: (A) suppression of PMA induced MMP-9 expression and their dose response; (B) densitometry analysis of MMP expression; (C) attenuation of VEGF expression in MDA-MB-231 cells after 24 h treatment; (D) cell viability (%) of cells after 72 h treatment. Results are presented as means ± SD; SD denoted by error bars (Experiments carried out in triplicate). $^{*}p < 0.05$.

of the active site (site A). A direct comparison of the dock scores at two different sites (i.e., site A and site B) implied that all the inhibitors exhibited a much higher dock score towards site B as compared to site A, indicating a reduced affinity of compounds for site A (Table S1, in Supplementary Information). Overlay of docked pose of all the inhibitors at site B revealed nearly identical binding orientations. Multiple weak interactions including H-bonding, cation-π, π-σ, *van der Waals* and hydrophobic interactions stabilized the protein-ligand association. In particular, the core scaffold of the compounds created a hydrogen-bonding network, whereas the phenyl rings were favoured to form hydrophobic interactions with the amino acid residues.

The docking orientations of the two most active compounds (**3c** and **4a**) were analyzed and compared with that of reference inhibitor, **7-DX**. The identified binding modes of **3c** and **4a** are depicted in Fig. 5a and b respectively. Compounds **3c** and **4a** exhibited a remarkably low binding affinity for site A (dock score 2.144 and 17.997 respectively) relative to site B (dock score 85.477 and 105.824 respectively). Compound **3c** appeared to form three hydrogen bonding interactions with Lys275, Ser471 and Ala469. On the other hand, compound **4a** constructed six hydrogen bonding contacts with different amino acid residues, including Ser471, Asp301, Asp304, Ala469 and Val427. It also created two cation-π interactions with Arg279 and Lys275, explaining its highest potency against enzyme. In addition, among all the compounds studied, compounds **4j** and **4k** with lipophilic groups (e.g. biphenyl and phenoxyphenyl) displayed the highest docking scores at site B and established themselves as potent TP inhibitors. Overall, the docking scores at site B were corroborating well with the experimental binding affinities of the compounds tested. Furthermore, compounds **3c** and **4a** conferred a better interaction than that of **7-DX** (dock score = 62.56 and 65.16 in site A and site B respectively). The reference inhibitor, **7-DX** was found to construct a hydrogen bonding network with Gly 271, Lys275 and Val 227, located at site B (Fig. S2, in Supplementary Information). By considering the results of the molecular modelling study, we can speculate that the compounds **3c** and **4a** may interact with the amino acid residues located at (site A) or adjacent (site B) to the active cleft [39] with a strong bonding force towards site B. Consequently, they showed a mixed mode of inhibition with respect to thymidine.

3. Conclusion

In conclusion, a small library of pyrazolo[1,5-*a*][1,3,5]triazine derivatives were synthesized *via* ring annelation reaction and assessed for their anti-TP activity. The biological evaluation identified a number of structurally distinct TP inhibitors. The most promising candidates (**3c** and **4a**) exhibited a mixed mode of inhibition towards TP. Moreover, selected TP inhibitors attenuated MMP-9 and VEGF expression in MDA-MB-231 cells, illustrating the

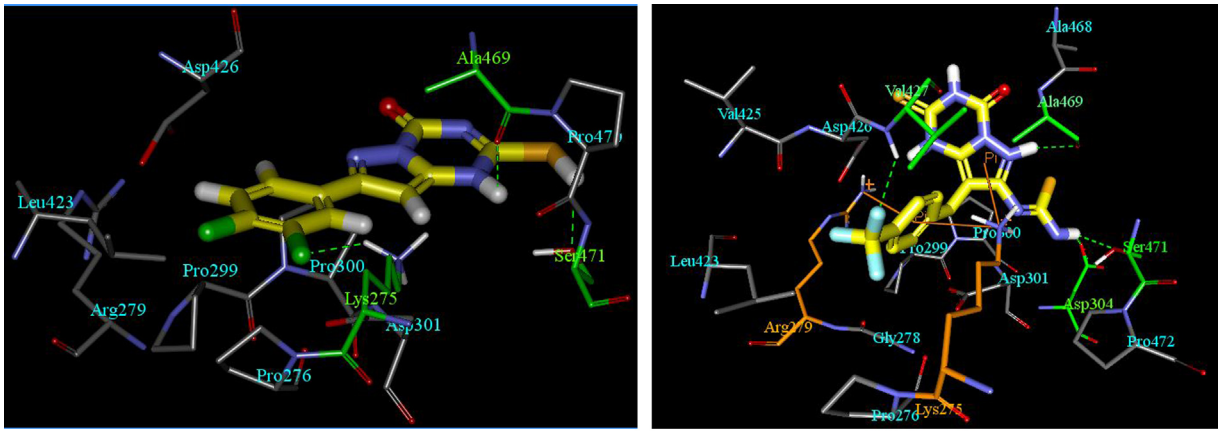

Fig. 5. Docked conformation of compounds **3c** (A) and **4a** (B) along with important amino acid residues in site B of TP (green dashed line indicates hydrogen bonding contacts, while brick red line implies π-cationic interactions with amino acid residues). (For interpretation of the references to colour in this figure legend, the reader is referred to the web version of this article.)

anti-angiogenic potential of these compounds. *In silico* docking study elucidated the distinct binding poses and interactions of these compounds to *enzyme*. Therefore, this study presents a starting point for the discovery of clinically useful novel TP inhibitors.

4. Experimental

4.1. Chemistry

4.1.1. General procedures

Commercially available reagents and solvents were used without further purification. Melting points were determined on a Gallenkamp melting point apparatus and were presented uncorrected. ^{1}H NMR and ^{13}C NMR spectra were recorded on a Bruker DPX-300 spectrometer at 300 MHz and 75 MHz respectively using DMSO-d_6 as solvent and TMS as internal standard. Mass spectra were obtained on a Finnigan MAT LCQ LC-MS mass spectrometer using electrospray ionization (ESI) mode. Reactions were monitored by TLC on silica gel (60 F_{254}) coated aluminium plate. The HPLC method was performed using Hewlett–Packard series 1050 HPLC system equipped with an HP-1050 quaternary pump, a degasser, diode array detector, an HP-1100 autosampler and a LiChrosorb reversed phase C18 (5 μm) column (4.6 × 250 mm). The separations were carried out using gradient elution. The experiment started using mobile phase composition of 95:5 (aqueous phase:acetonitrile) which gradually changed to 0:100 within 7 min. The flow rate was set at 1 mL/min and the ultraviolet detection was made at wavelength 254 nm. Elemental analyses were carried out on a Vario EL-III C, H, N, S analyzer (Germany) and values were within ±0.5% of the calculated values. The purity of all synthesized compounds was found to be more than 95%.

4.1.2. General procedure for the synthesis of 2-thioxo-pyrazolo[1,5-a][1,3,5]triazin-4-ones (**3-3c** and **4-4n**)

Initially, cyanoacetophenones (**6**) were accomplished through the reaction of substituted bromoacetophenones (**5**) (10 mmol) with sodium cyanide (20 mmol). 5-aminopyrazoles (**7**) were then prepared from the cyclocondensation of cyanoacetophenones (**6**) (10 mmol) with hydrazine (20 mmol) under microwave irradiation [26,27]. Moreover, 3,5-diaminopyrazoles (**11**) were synthesized *via* an initial formation of mono-substituted malononitriles (**10**) from the condensation of substituted aromatic or heteroaromatic aldehydes (**9**) (10 mmol) with malononitrile (10 mmol), as described previously [28]. The resulting mono-substituted malononitriles (**10**) (10 mmol) were subsequently treated with hydrazine hydrate (20 mmol) in refluxing ethanol to obtain 3,5-diaminopyrazoles (**11**). In the next step, the reactions between 5-aminopyrazoles (**7**)/3,5-diaminopyrazoles (**11**) (3 mmol) and ethoxycarbonyl isothiocyanate (3.3 mmol) in anhydrous DMF (4 mL) at room temperature yielded corresponding thiourea (**8** and **12**) derivatives.

To a stirred solution of sodium hydroxide (9 mmol) in ethanol (80%, 20 mL), carbethoxythiourea derivatives (**8** and **12**) (3 mmol) were added and heated on a water bath for 20 min. After cooling, the solvent was slowly evaporated under vacuum, and the residue was suspended in water (25 mL). The resulting suspension was then acidified up to pH 1–3 using 2.5 M HCl. The precipitated products (**3-3c** and **4-4n**) was filtered off, purified with an appropriate solvent, and dried under vacuum (Schemes 1 and 2).

4.1.3. 7-Phenyl-2-thioxo-2,3-dihydro-1H-pyrazolo[1,5-a][1,3,5] triazin-4-one (**3**)

White powder (71% yield); Mp 285–286 °C (Ethanol-water); ESI-MS *m*/*z* 243.0 $(M-1)^+$; ^{1}H NMR (300 MHz, DMSO-*d6*): δ 6.39 (s, 1H, CH), 7.38–7.54 (m, 3H, H-3′, H-4′ and H-5′), 7.88–8.00 (m, 2H, H-2′ and H-6′), 12.75 (s, 1H, NH), 13.56 (s, 1H, NH); ^{13}C NMR (75 MHz, DMSO-*d6*): δ 87.3 (C-8), 126.8 (C-3′ and C-5′), 129.4 (C-2′ and C-6′), 130.1 (C-4′), 131.7 (C-1′), 142.0 (C-7), 142.1 (C-9), 155.9 (C-4), 173.6 (C-2); Anal. calcd. for $C_{11}H_8N_4OS$: C, 54.09; H, 3.30; N, 22.94. Found: C, 53.78; H, 3.24; N, 22.74.

4.1.4. 7-t-Butyl-2-thioxo-2,3-dihydro-1H-pyrazolo[1,5-a][1,3,5] triazin-4-one (**3a**)

White powder (55% yield); Mp 268–270 °C (Ethanol-water); ESI-MS *m*/*z* 223.1 $(M-1)^+$; ^{1}H NMR (300 MHz, DMSO-*d6*): δ 1.23 (s, 9H, t-but), 5.83 (s, 1H, CH), 12.59 (s, 1H, NH), 13.37 (s, 1H, NH). ^{13}C NMR (75 MHz, DMSO-*d6*): δ 30.1 ($3CH_3$), 33.0 (t-but), 87.1 (C-8), 141.1 (C-7), 142.0 (C-9), 167.5 (C-4), 173.4 (C-2); Anal. calcd. for $C_9H_{12}N_4OS$: C, 48.20; H, 5.39; N, 24.98. Found: C, 47.42; H, 5.32; N, 24.52.

4.1.5. 7-(4-Cyano-phenyl)-2-thioxo-2,3-dihydro-1H-pyrazolo[1,5-a][1,3,5]triazin-4-one (**3b**)

White powder (61% yield); Mp > 300 °C (Ethanol-water); ESI-MS *m*/*z* 287.2 $(M-1)^+$; ^{1}H NMR (300 MHz, DMSO-*d6*): δ 6.50 (s,

1H, CH), 7.97–8.16 (m, 4H, Ar–H), 12.82 (s, 1H, NH), 13.64 (s, 1H, NH). ^{13}C NMR (75 MHz, DMSO-*d6*): δ 87.6–87.7 (C-8), 126.6–126.8 (C-2′ and C-6′), 128.6–130.4 (C-3′ and C-5′), 131.9 (C-4′), 134.3 (CN), 135.5–135.8 (C-1′), 142.0–142.3 (C-7), 154.9–155.1 (C-9), 167.4–167.9 (C-4), 173.6 (C-2); Anal. calcd. for $C_{12}H_7N_5OS$: C, 53.52; H, 2.62; N, 26.01. Found: C, 52.88; H, 2.57; N, 26.42.

4.1.6. 7-(3,4-Dichloro-phenyl)-2-thioxo-2,3-dihydro-1H-pyrazolo [1,5-a][1,3,5]triazin-4-one (**3c**)

White powder (63% yield); Mp 287–289 °C (Ethanol-water); ESI-MS *m*/*z* 312.9 $(M-1)^+$; ^{1}H NMR (300 MHz, DMSO-*d6*): δ 6.52 (s, 1H, CH), 7.71 (d, 1H, H-6′, *J* = 8.3 Hz), 7.94 (dd, 1H, H-5′, *J* = 8.5 Hz, *J* = 2.1 Hz), 8.18 (d, 1H, H-2′, *J* = 1.9 Hz), 12.80 (s, 1H, NH), 13.63 (s, 1H, NH). ^{13}C NMR (75 MHz, DMSO-*d6*): δ 87.7 (C-8), 126.7 (C-6′), 128.4 (C-2′), 131.6 (C-5′), 132.3 (C-4′), 132.4 (C-3′), 132.5 (C-1′), 141.9 (C-7), 142.3 (C-9), 153.6 (C-4), 173.6 (C-2); Anal. calcd. for $C_{11}H_6Cl_2N_4OS$: C, 42.19; H, 1.93; N, 17.89. Found: C, 42.65; H, 1.88; N, 17.42.

4.1.7. (8-Benzyl-4-oxo-2-thioxo-1,2,3,4-tetrahedro-pyrazolo[1,5-a] [1,3,5]triazin-7-yl)-thiourea (**4**)

White powder (73% yield); Mp 239–241 °C (Ethanol-water); ESI-MS *m*/*z* 331.1 $(M-1)^+$; ^{1}H NMR (30 MHz, DMSO-*d6*): δ 4.11(s, 2H, CH_2), 7.12–7.33 (m, 5H, Ph), 8.94 and 9.07 (2 s, 2H, (C=S) NH_2), 10.06 (s, 1H, (C=S) NH), 12.70 (s, 1H, N_H), 13.57 (br. s, 1H, NH); ^{13}C NMR (75 MHz, DMSO-*d6*): δ 24.2 (CH_2), 92.0 (C-8), 125.8 (C-4′), 127.8 (C-3′ and C-5′), 128.2 (C-2′and C-6′), 138.5 (C-1′), 139.6 (C-7), 140.7 (C-9), 151.9 (C-4), 173.5 (C-2), 179.8 (NH(C=S)NH_2); Anal. calcd. for $C_{13}H_{12}N_6OS_2$: C, 46.97; H, 3.64; N, 25.28. Found: C, 45.85; H, 3.52; N, 24.89.

4.1.8. [8-(4-Trifluoromethyl-benzyl)-4-oxo-2-thioxo-1,2,3,4-tetrahedro-pyrazolo[1,5-a][1,3,5]triazin-7-yl]-thiourea (**4a**)

White powder (71% yield); Mp 189–191 °C (Ethanol-water); ESI-MS *m*/*z* 399. $(M-1)^+$; ^{1}H NMR (300 MHz, DMSO-*d6*): δ 4.21 (s, 2H, CH_2), 7.39 (d, 2H, H-3′ and H-5′, *J* = 7.9 Hz), 7.65 (d, 2H, H-2′ and H-6′, *J* = 8.1 Hz), 8.95 and 9.10 (2 s, 2H, (C=S) NH_2), 10.21 (s, 1H, (C=S) NH), 12.65 (s, 1H, NH), 13.53 (br. s, 1H, NH); ^{13}C NMR (75 MHz, DMSO-*d6*): δ 24.4 (CH_2), 91.0 (C-8), 124.4 (q, CF_3, *J* = 271.9 Hz), 124.9 (q, C-3′ and C-5′, *J* = 3.7 Hz), 126.7 (q, C-4′, *J* = 31.5 Hz), 128.6 (C-2′and C-6′), 139.3 (C-1′), 140.9 (C-7), 144.8 (C-9), 151.9 (C-4), 173.6 (C-2), 179.9 (NH(C=S)NH_2); Anal. calcd. for $C_{14}H_{11}F_3N_6OS_2$: C, 42.00; H, 2.77; N, 20.99. Found: C, 43.24; H, 2.68; N, 20.79.

4.1.9. [8-(4-Chloro-benzyl)-4-oxo-2-thioxo-1,2,3,4-tetrahedro-pyrazolo[1,5-a][1,3,5]triazin-7-yl]-thiourea (**4b**)

White powder (78% yield); Mp 243–245 °C (Ethanol-water); ESI-MS *m*/*z* 365.1 $(M-1)^+$; ^{1}H NMR (300 MHz, DMSO-*d6*): δ 4.09 (s, 2H, CH_2), 7.18 (d, 2H, H-3′ and H-5′, *J* = 8.4 Hz), 7.33 (d, 2H, H-2′ and H-6′, *J* = 8.5 Hz), 8.94 and 9.05 (2 s, 2H, (C=S) NH_2), 10.11 (s, 1H, (C=S) NH), 12.69 (s, 1H, NH), 13.53 (br. s, 1H, NH); ^{13}C NMR (75 MHz, DMSO-*d6*): δ 23.7 (CH_2), 91.6 (C-8), 128.0 (C-3′ and C-5′), 129.7 (C-2′and C-6′), 130.4 (C-4′), 138.7 (C-1′), 138.7 (C-7), 140.7 (C-9), 151.8 (C-4), 173.5 (C-2), 179.8 (NH(C=S)NH_2); Anal. calcd. for $C_{13}H_{11}ClN_6OS_2$: C, 42.56; H, 3.02; N, 22.91. Found: C, 42.12; H, 3.11; N, 22.08.

4.1.10. [8-(4-Bromo-benzyl)-4-oxo-2-thioxo-1,2,3,4-tetrahedro-pyrazolo[1,5-a][1,3,5]triazin-7-yl]-thiourea (**4c**)

White powder (82% yield); Mp 220 °C (Ethanol-water); ESI-MS *m*/*z* 411.1 $(M-1)^+$; ^{1}H NMR (300 MHz, DMSO-*d6*): δ 4.07 (s, 2H, CH_2), 7.13 (d, 2H, H-3′ and H-5′, *J* = 8.4 Hz), 7.46 (d, 2H, H-2′ and H-6′, *J* = 8.4 Hz), 8.93 and 9.05 (2 s, 2H, (C=S) NH_2), 10.09 (s, 1H, (C=S) NH), 12.67 (s, 1H, NH), 13.52 (br. s, 1H, NH); ^{13}C NMR (75 MHz, DMSO-*d6*): δ 23.8 (CH_2), 91.6 (C-8), 118.9 (C-4′), 130.2 (C-3′ and C-5′), 131.0 (C-2′and C-6′), 138.8 (C-1′), 139.2 (C-7), 140.8 (C-9), 151.9 (C-4), 173.6 (C-2), 179.9 (NH(C=S)NH_2); Anal. calcd. for $C_{13}H_{11}BrN_6OS_2$: C, 37.96; H, 2.70; N, 20.43. Found: C, 37.32; H, 2.65; N, 20.52.

4.1.11. [8-(4-Fluoro-benzyl)-4-oxo-2-thioxo-1,2,3,4-tetrahedro-pyrazolo[1,5-a][1,3,5]triazin-7-yl]-thiourea (**4d**)

White powder (65% yield); Mp 221–223 °C (Ethanol-water); ESI-MS *m*/*z* 349.0 $(M-1)^+$; ^{1}H NMR (300 MHz, DMSO-*d6*): δ 4.09 (s, 2H, CH_2), 7.10 (dd, 2H, H-3′ and H-5′, *J* = 8.9, 8.9 Hz), 7.20 (dd, 2H, H-2′ and H-6′, *J* = 8.7, 5.6 Hz), 8.94 and 9.05 (2 s, 2H, (C=S) NH_2), 10.09 (s, 1H, (C=S) NH), 12.69 (s, 1H, NH), 13.55 (br. s, 1H, NH); ^{13}C NMR (75 MHz, DMSO-*d6*): δ 23.4 (CH_2), 92.7 (C-8), 114.8 (d, C-3′ and C-5′, *J* = 21.3 Hz), 129.6 (d, C-2′ and C-6′, *J* = 7.3 Hz), 135.7 (d, C-1′, *J* = 2.9 Hz), 138.6 (C-7), 140.8(C-9), 151.8(C-4), 160.6 (d, C-4′, *J* = 241.4 Hz), 173.5(C-2), 179.8 (NH(C=S)NH_2); Anal. calcd. for $C_{13}H_{11}FN_6OS_2$: C, 44.56; H, 3.16; N, 23.98. Found: C, 43.26; H, 3.22; N, 22.76.

4.1.12. [8-(4-Methyl-benzyl)-4-oxo-2-thioxo-1,2,3,4-tetrahedro-pyrazolo[1,5-a][1,3,5]triazin-7-yl]-thiourea (**4e**)

White powder (76% yield); Mp 254–256 °C (Ethanol-water); ESI-MS *m*/*z* 345.1 $(M-1)^+$; ^{1}H NMR (300 MHz, DMSO-*d6*): δ 2.25 (s, 3H, Me), 4.05 (s, 2H, CH_2), 7.04–7.09 (m, 5H, Ar–H), 8.93 and 9.03 (2 s, 2H, (C=S) NH2), 9.98 (s, 1H, (C=S) NH), 12.69 (s, 1H, NH), 13.55 (br. s, 1H, NH); ^{13}C NMR (75 MHz, DMSO-*d6*): δ 20.5 (Me), 23.7 (CH_2), 92.4 (C-8), 112.7 (C-3′ and C-5′), 128.7 (C-2′and C-6′), 134.8 (C-4′), 136.4 (C-1′), 138.3 (C-7), 140.7 (C-9), 151.9 (C-4), 173.5 (C-2), 179.7 (NH(C=S)NH_2); Anal. calcd. for $C_{14}H_{14}N_6OS_2$: C, 48.54; H, 4.07; N, 24.26. Found: C, 47.26; H, 3.98; N, 24.54.

4.1.13. [8-(4-Ethyl-benzyl)-4-oxo-2-thioxo-1,2,3,4-tetrahedro-pyrazolo[1,5-a][1,3,5]triazin-7-yl]-thiourea (**4f**)

White powder (73% yield); Mp 240 °C (Ethanol-water); ESI-MS *m*/*z* 359.1 $(M-1)^+$; ^{1}H NMR (300 MHz, DMSO-*d6*): δ 1.14 (t, 3H, CH_3, *J* = 7.6 Hz), 2.55 (q, 2H, CH_2, *J* = 7.6 Hz), 4.05 (s, 2H, CH_2), 7.07 (d, 2H, H-3′ and H-5′, *J* = 8.3 Hz), 7.11 (d, 2H, H-2′ and H-6′, *J* = 8.5 Hz), 8.94 and 9.07 (2 s, 2H, (C=S) NH_2), 10.03 (s, 1H, (C=S) NH), 12.63 (s, 1H, NH), 13.54 (br. s, 1H, NH); ^{13}C NMR (75 MHz, DMSO-d6): δ 15.7 (Me), 23.8 (CH_2), 27.7 (CH_2), 92.4 (C-8), 127.5 (C-3′ and C-5′), 127.8 (C-2′and C-6′), 136.8 (C-4′), 138.6 (C-1′), 140.8 (C-7), 141.2 (C-9), 151.9 (C-4), 173.5 (C-2), 179.8 (NH(C=S)NH_2); Anal. calcd. for $C_{15}H_{16}N_6OS_2$: C, 49.98; H, 4.47; N, 23.31. Found: C, 48.84; H, 4.42; N, 23.02.

4.1.14. [8-(4-Methoxy-benzyl)-4-oxo-2-thioxo-1,2,3,4-tetrahedro-pyrazolo[1,5-a][1,3,5]triazin-7-yl]-thiourea (**4g**)

White powder (69%); Mp 252–254 °C (Ethanol-water); ESI-MS *m*/*z* 361.1 $(M-1)^+$; ^{1}H NMR (300 MHz, DMSO-*d6*): δ 3.71 (s, 3H, OMe), 4.03 (s, 2H, CH_2), 6.84 (d, 2H, H-3′ and H-5′, *J* = 8.8 Hz), 7.10 (d, 2H, H-2′ and H-6′, *J* = 8.7 Hz), 8.95 and 9.04 (2 s, 2H, (C=S) NH_2), 9.99 (s, 1H, (C=S) NH), 12.70 (s, 1H, NH), 13.56 (br. s, 1H, NH); ^{13}C NMR (75 MHz, DMSO-*d6*): δ 23.3 (CH2), 54.9 (MeO), 92.7 (C-8), 113.6 (C-3′ and C-5′), 128.8 (C-2′ and C-6′), 131.4 (C-4′), 138.2 (C-1′), 140.7 (C-7), 151.9 (C-9), 157.5 (C-4), 173.5 (C-2), 179.7 (NH(C=S) NH_2); Anal. calcd. for $C_{14}H_{14}N_6O_2S_2$: C, 46.40; H, 3.89; N, 23.19. Found: C, 46.12; H, 3.82; N, 23.11.

4.1.15. [8-(4-Hydroxy-benzyl)-4-oxo-2-thioxo-1,2,3,4-tetrahedro-pyrazolo[1,5-a][1,3,5]triazin-7-yl]-thiourea (**4h**)

White powder (80% yield); Mp 219–221 °C (Ethanol-water); ESI-MS *m*/*z* 347.1 $(M-1)^+$; ^{1}H NMR (300 MHz, DMSO-*d6*): δ 3.97 (s, 2H, CH_2), 6.66 (d, 2H, H-3′ and H-5′, *J* = 8.5 Hz), 6.96 (d, 2H, H-2′ and H-6′, *J* = 8.5 Hz), 8.94 and 9.03 (2 s, 2H, (C=S) NH_2), 9.17 (s, 1H, OH),

9.90 (s, 1H, (C=S) NH), 12.68 (s, 1H, NH), 13.54 (br. s, 1H, NH); ^{13}C NMR (75 MHz, DMSO-*d6*): δ 23.3 (CH_2), 92.7 (C-8), 114.9 (C-3′ and C-5′), 128.7 (C-2'and C-6′), 129.5 (C-4′), 138.2 (C-1′), 140.7 (C-7), 151.9 (C-9), 155.4 (C-4), 173.5 (C-2), 179.7 (NH(C=S)NH_2); Anal. calcd. for $C_{13}H_{12}N_6O_2S_2$: C, 44.82; H, 3.47; N, 24.12. Found: C, 44.26; H, 3.39; N, 23.76.

*4.1.16. [8-(4-Cyano-benzyl)-4-oxo-2-thioxo-1,2,3,4-tetrahedro-pyrazolo[1,5-a][1,3,5]triazin-7-yl]-thiourea (**4i**)*

White powder (62% yield); Mp 252–254 °C (Ethanol-water); ESI-MS *m/z* 356.1 $(M-1)^+$; ^{1}H NMR (300 MHz, DMSO-*d6*): δ 4.20 (s, 2H, CH_2), 7.34 (d, 2H, H-3′ and H-5′, *J* = 8.3 Hz), 7.46 (d, 2H, H-2′ and H-6′, *J* = 8.3 Hz), 8.96 and 9.06 (2 s, 2H, (C=S) NH_2), 10.22 (s, 1H, (C=S) NH), 12.74 (s, 1H, NH), 13.55 (br. s, 1H, NH); ^{13}C NMR (75 MHz, DMSO-*d6*): δ 24.7 (CH_2), 90.6 (C-8), 108.7 (CN), 118.9 (C-4′), 128.9 (C-3′ and C-5′), 132.0 (C-2'and C-6′), 138.9 (C-1′), 140.8 (C-7), 145.8 (C-9), 151.8 (C-4), 173.6 (C-2), 179.7 (NH(C=S)NH_2); Anal. calcd. for $C_{14}H_{11}N_7OS_2$: C, 47.05; H, 3.10; N, 27.43. Found: C, 46.76; H, 3.14; N, 27.98.

*4.1.17. (8-Biphenyl-4-ylmethyl-4-oxo-2-thioxo-1,2,3,4-tetrahedro-pyrazolo[1,5-a][1,3,5]triazin-7-yl)-thiourea (**4j**)*

White powder (70%); Mp 246–248 °C (Ethanol-water); ESI-MS *m/z* 407.1 $(M-1)^+$; ^{1}H NMR (300 MHz, DMSO-*d6*): δ 4.16 (s, 2H, CH_2), 7.27 (d, 2H, H-3″ and H-5″, *J* = 8.2 Hz), 7.33 (t, 1H, H-4″, *J* = 7.3 Hz), 7.44 (t, 2H, H-2″ and H-6″, *J* = 7.7 Hz), 7.58 (d, 2H, H-3′ and H-5′, *J* = 8.2 Hz), 7.63 (d, 2H, H-2′ and H-6′, *J* = 7.5 Hz), 8.98 and 9.12 (2 s, 2H, (C=S) NH_2), 10.15 (s, 1H, (C=S) NH), 12.67 (s, 1H, NH), 13.52 (br. s, 1H, NH). ^{13}C NMR (75 MHz, DMSO-*d6*): δ 23.9 (CH_2), 92.0 (C-8), 126.4 (C-3′ and C-5′), 126.5 (C-2′ and C-6′), 127.1 (C-4′), 128.4 (C-3″ and C-5″), 128.8 (C-2″and C-6″), 137.8 (C-1′), 138.8 (C-4″), 139.0 (C-1″), 139.9 (C-7), 140.8 (C-9), 151.9 (C-4), 173.6 (C-2), 179.8 (NH(C=S)NH_2); Anal. calcd. for $C_{19}H_{16}N_6OS_2$: C, 55.86; H, 3.95; N, 20.57. Found: C, 54.78; H, 3.87; N, 21.28.

*4.1.18. [4-Oxo-8-(4-phenoxy-benzyl)-2-thioxo-1,2,3,4-tetrahedro-pyrazolo[1,5-a][1,3,5]triazin-7-yl]-thiourea (**4k**)*

White powder (81%); Mp 210–212 °C (Ethanol-water); ESI-MS *m/z* 423.2 $(M-1)^+$; ^{1}H NMR (300 MHz, DMSO-*d6*): δ 4.09 (s, 2H, CH_2), 6.81–7.45 (m, 9H, Ar–H), 8.96 and 9.07 (2 s, 2H, (C=S) NH_2), 10.07 (s, 1H, (C=S) NH), 12.68 (s, 1H, NH), 13.53 (br. s, 1H, NH); ^{13}C NMR (75 MHz, DMSO-d6): δ 23.6 (CH_2), 92.1 (C-8), 118.1 (C-3′ and C-5′), 118.6 (C-2′ and C-6′), 123.0 (C-4′), 129.4 (C-3″ and C-5″), 129.9 (C-2″and C-6″), 134.8 (C-1′), 138.6 (C-4″), 140.8 (C-1″), 151.9 (C-7), 154.6 (C-9), 156.9 (C-4), 173.5 (C-2), 179.8 (NH(C=S)NH_2); Anal. calcd. for $C_{19}H_{16}N_6O_2S_2$: C, 53.76; H, 3.80; N, 19.80. Found: C, 54.22; H, 3.72; N, 20.21.

*4.1.19. (8-Naphthalen-2-ylmethyl-4-oxo-2-thioxo-1,2,3,4-tetrahedropyrazolo[1,5-a][1,3,5]triazin-7-yl]-thiourea (**4l**)*

White powder (63% yield); Mp 230–233 °C (Ethanol-water); ESI-MS *m/z* 381.2 $(M-1)^+$; ^{1}H NMR (300 MHz, DMSO-*d6*): δ 4.56 (s, 2H, CH_2), 6.85–6.26 (m, 11H, Ar–H), 9.00 and 9.26 (2 s, 2H, (C=S) NH_2), 10.22 (s, 1H, (C=S) NH), 12.72 (s, 1H, NH), 13.48 (br. s, 1H, NH); ^{13}C NMR (75 MHz, DMSO-*d6*): δ 22.2 (CH_2), 90.0 (C-8), 123.1 (Ar–C), 123.8 (Ar–C), 125.5 (Ar–C), 125.6 (Ar–C), 125.7 (Ar–C), 126.2 (Ar–C), 128.2 (Ar–C), 131.5 (Ar–C), 133.1 (Ar–C), 135.4 (Ar–C), 139.1 (C-7), 140.8 (C-9), 152.6 (C-4), 173.5 (C-2), 179.9 (NH(C=S) NH_2); Anal. calcd. for $C_{17}H_{14}N_6OS_2$: C, 53.39; H, 3.69; N, 21.97. Found: C, 52.75; H, 3.62; N, 21.45.

*4.1.20. (8-Furan-2-ylmethyl-4-oxo-2-thioxo-1,2,3,4-tetrahedro-pyrazolo[1,5-a][1,3,5]triazin-7-yl]-thiourea (**4m**)*

White powder (74% yield); Mp 227–229 °C (Ethanol-water); ESI-MS *m/z* 321.0 $(M-1)^+$; ^{1}H NMR (300 MHz, DMSO-*d6*): δ 4.13 (s, 2H, CH_2), 6.00 (d, 1H, H-3′, *J* = 3.1 Hz), 6.34 (dd, 1H, H-4′, *J* = 3.1, 1.9 Hz), 7.55 (d, 1H, H-5′, *J* = 1.0 Hz), 8.98 and 9.09 (2 s, 2H, (C=S) NH_2), 10.12 (s, 1H, (C=S) NH), 12.72 (s, 1H, NH), 13.54 (br. s, 1H, NH); ^{13}C NMR (75 MHz, DMSO-*d6*): δ 18.5 (CH_2), 89.2 (C-8), 105.5 (C-4′), 110.4 (C-3′), 138.5 (C-5′), 140.7 (C-2′), 141.6 (C-7), 151.8 (C-9), 152.9 (C-4), 173.5 (C-2), 179.8 (NH(C=S) NH_2); Anal. calcd. for $C_{11}H_{10}N_6O_2S_2$: C, 40.98; H, 3.13; N, 26.07. Found: C, 40.18; H, 3.21; N, 27.24.s

*4.1.21. (4-Oxo-8-thiophen-2-ylmethyl-2-thioxo-1,2,3,4-tetrahedro-pyrazolo[1,5-a][1,3,5]triazin-7-yl]-thiourea (**4n**)*

White powder (72% yield); Mp 230–232 °C (Ethanol-water); ESI-MS *m/z* 337.0 $(M-1)^+$; ^{1}H NMR (300 MHz, DMSO-*d6*): δ 4.30 (s, 2H, CH_2), 6.81 (d, 1H, H-3′, *J* = 2.8 Hz), 6.92 (dd, 1H, H-4′, *J* = 5.0, 3.5 Hz), 7.32 (d, 1H, H-5′, *J* = 5.0 Hz), 8.97 and 9.06 (2 s, 2H, (C=S) NH_2), 10.19 (s, 1H, (C=S) NH), 12.72 (s, 1H, NH), 13.61 (br. s, 1H, NH); ^{13}C NMR (75 MHz, DMSO-*d6*): δ 19.4 (CH_2), 92.1 (C-8), 124.0 (C-4′), 124.5 (C-5′), 126.7 (C-3′), 138.2 (C-2′), 140.7 (C-7), 142.6 (C-9), 151.6 (C-4), 173.5 (C-2), 179.8 (NH(C=S) NH_2); Anal. calcd. for $C_{11}H_{10}N_6OS_3$: C, 39.04; H, 2.98; N, 24.83. Found: C, 40.22; H, 3.92; N, 24.06.

4.2. Biological characterisation

4.2.1. In vitro thymidine phosphorylase enzyme assay

A spectrophotometric assay method [29] was adopted to evaluate *in vitro* TP inhibitory activity of the synthesized compounds. Briefly, thymidine (substrate) and recombinant thymidine phosphorylase, expressed in E. coli (T2807-Sigma) were utilized for this assay. The enzymatic reaction was initiated by the addition of substrate (200 μL, 5 mM) into a cuvette containing 780 μl of potassium phosphate buffer (pH 7.4), 10 μL of enzyme at concentration of 1.5 U, and 10 μL of test compounds dissolved in DMSO. The conversion of thymidine to thymine was determined at 290 nm after 4, 8, 12, 16 and 20 min on a Shimadzu UV Mini 1240 UV–Vis Spectrophotometer. The initial rates of change in absorbance at different concentrations of inhibitor were converted to % inhibition of enzyme. *Plotting* the data as *% inhibition* as a function of *inhibitor concentration* using Graphpad Prism vs 4.0 yielded the IC_{50} values. The slope of uninhibited enzyme was estimated by conducting same experiments using 10 μL of DMSO. The percentage activity of each inhibitor was calculated by the following equations-

(i) Activity = (Slope of inhibited enzyme/Slope of uninhibited enzyme) × 100%
(ii) Inhibition = 100% − Activity

All the experiments were carried out in triplicate.

4.2.2. Enzyme inhibition kinetics study

The enzyme inhibition was evaluated in the presence of different concentrations of inhibitor at varying concentrations of thymidine (1000, 500, 300, 200, 100 μM). The inorganic phosphate was *fixed at* **the** *saturating concentration* (25 mM). The conversion of thymidide (dThd) to thymine was recorded at 290 nm. All the experiments were conducted in triplicate.

4.2.3. Gelatine zymography

Gelatine zymography was preformed following reported procedures with some modifications (Liotta and Stetler-Stevenson 1990) [35]. Briefly, the MDA-MB-231 cells were seeded onto six-well plates in RPMI with 10% FBS and allowed to grow to 80% confluence. The cells were passaged into serum-free medium for at least 24 h before being treated with compounds and PMA (80 nM). After incubation, the conditioned medium was harvested and then

assayed for protein content. The volume of each samples having equal amount of protein was adjusted by adding PBS to samples. The resulting samples were mixed with 3× loading buffer and subjected to electrophoresis on a 7.5% SDS-PAGE gel containing 0.1% (w/v) gelatine using 1× Tris-Glycin SDS running buffer at 100 V for 90–120 min. Subsequently, the gels were placed in renaturing buffer (2.5% Triton X-100), *washed thoroughly* to remove traces of SDS and equilibrated in 1× zymogram developing buffer (50 mM tris, 10 mM $CaCl_2$, 0.15 M NaCl, pH-7.5). The gels were then incubated overnight at 37 °C in fresh developing buffer to allow gelatine digestion. The gelatinolytic activity of MMPs was visualized by staining the gels with 1% coomassie blue R-250 and destained repeatedly in 50% methanol, 10% acetic acid, 40% water (v/v) until the bands were clearly visible.

4.2.4. VEGF assay

The VEGF expression in MDA-MB-231 cells was assessed *with a colorimetric enzyme-linked* immunosorbent assay (ELISA) kit following the manufacturer's instructions. (Abfrontier) [15]. After treatment with the indicated doses of compounds or DMSO, the cell supernatant was collected and subjected to centrifugation (5000 g for 5 min) to remove cells and debris. The diluted samples and VEGF standard solutions were placed in the precoated 96-well plate and incubated at 37 °C for 90 min. Subsequently, the plate contents were discarded and 0.1 mL of biotinylated anti-human VEGF antibody working solution was introduced and incubated for another 60 min. The plates were then thoroughly washed with 0.01 M TBS and 0.1 mL of avidin-biotin-peroxidase complex working solution was added to each well. After 30 min of incubation, 90 μL of prepared TMB colour developing solution was poured into each well and incubated at 37 °C for an additional 25 min. The reactions were stopped by adding 0.1 mL of prepared TMB stop solution to each well and the absorbance was then measured at 450 nm.

4.2.5. MTT assay

MTT (3-(4,5-dimethylthiazol-2-yl)-2,5-diphenyl tetrazolium bromide) colorimetric assay (Alley et al., 1988) [36] was adopted to evaluate the cytotoxicity of the synthesized compounds in MDA-MB-231cells. Briefly, cells grown to 80% confluence were seeded at a density of 5000 cells/well in 96-well plates and were incubated for 24 h. The cells were then treated with the indicated doses of compounds and incubated for another 72 h. Subsequently, the cells were incubated for 4 h with MTT solution (50 μL). The *absorbance* at *570 nm* was *recorded* using a microplate reader. The effect of compounds on cell viability was expressed as percent cell viability and compared with the vehicle treated control cells.

4.2.6. Densitometric and statistical analysis

Band intensities were quantified with Image Gauge 4.0 software. The numerical data were presented as mean ± standard deviation. Statistical significance between treatment and control groups was analyzed using ANOVA test. A value of $P > 0.05$ was reported as statistically significant.

4.3. Molecular docking study

In *silico* docking studies were performed using the LigandFit module implemented in the Accelrys Discovery Studio 2.1 (Accelrys Inc, San Diego, CA, USA) [38]. The co-crystal structure of the protein and ligand (5-iodouracil, **5-IUR**) was retrieved from protein data bank (PDB ID: 2WK6) [37]. The protein was prepared by deleting the identical B chain, unwanted water molecules and adding hydrogens. It was further energy minimized by using the CHARMM force field. The idealized active site was selected based on the ligand binding domain. For ligand preparation, all the duplicate structures were removed and options for tautomer generation, ionization change, isomer generation and 3D-generator were set to the default values. Subsequently, molecular docking of the pre-processed ligands was performed and various binding conformations for ligands were generated by Monte Carlo trial method. The final energy refinement of the ligand pose or pose optimization in ligandfit was estimated with Broyden-Flecher Gold Farbshanno (BFGS) method. The *best-scoring docking pose* of each ligand was identified and the dock scores were *compared with the* experimental *binding* affinities.

Acknowledgements

This work was financially supported by National Medical Research Council Grant, Singapore (R-148-000-102-275) and Academic Research Funds of National University of Singapore. The authors are also thankful to Gokaraju Rangaraju Educational Society and Jadavpur University for constant encouragement and for providing essential laboratory facilities for this project.

Appendix A. Supplementary data

Supplementary data related to this article can be found at http://dx.doi.org/10.1016/j.ejmech.2014.03.063. These data include MOL files and InChiKeys of the most important compounds described in this article.

References

[1] P. Pisani, D.M. Parkin, F. Bray, J. Ferlay, Estimates of the worldwide mortality from 25 cancers in 1990, International Journal of Cancer 83 (1999) 18–29.
[2] J. Folkman, E. Merler, C. Abernathy, G. Williams, Isolation of a tumor factor responsible or angiogenesis, Journal of Experimental Medicine 133 (1971) 275–288.
[3] L. Hlatky, P. Hahnfeldt, J. Folkman, Clinical application of antiangiogenic therapy: microvessel density, what it does and doesn't tell us, Journal of the National Cancer Institute 94 (2002) 883–893.
[4] N. Weidner, J.P. Semple, W.R. Welch, J. Folkman, Tumor angiogenesis and metastasis – correlation in invasive breast carcinoma, New England Journal of Medicine 324 (1991) 1–8.
[5] J. Folkman, Tumor angiogenesis: therapeutic implications, New England Journal of Medicine 285 (1971) 1182–1186.
[6] F. Haviv, M.F. Bradley, D.M. Kalvin, A.J. Schneider, D.J. Davidson, S.M. Majest, L.M. McKay, C.J. Haskell, R.L. Bell, B. Nguyen, K.C. Marsh, B.W. Surber, J.T. Uchic, J. Ferrero, Y.-C. Wang, J. Leal, R.D. Record, J. Hodde, S.F. Badylak, R.R. Lesniewski, J. Henkin, Thrombospondin-1 mimetic peptide inhibitors of angiogenesis and tumor growth: design, synthesis, and optimization of pharmacokinetics and biological activities, Journal of Medicinal Chemistry 48 (2005) 2838–2846.
[7] G. Bold, K.-H. Altmann, J. Frei, M. Lang, P.W. Manley, P. Traxler, B. Wietfeld, J. Brüggen, E. Buchdunger, R. Cozens, S. Ferrari, P. Furet, F. Hofmann, G. Martiny-Baron, J. Mestan, J. Rösel, M. Sills, D. Stover, F. Acemoglu, E. Boss, R. Emmenegger, L. Lässer, E. Masso, R. Roth, C. Schlachter, W. Vetterli, D. Wyss, J.M. Wood, New anilinophthalazines as potent and orally well absorbed inhibitors of the VEGF receptor tyrosine kinases useful as antagonists of tumor-driven angiogenesis, Journal of Medicinal Chemistry 43 (2000) 2310–2323.
[8] M.T. Conconi, G. Marzaro, L. Urbani, I. Zanusso, R. Di Liddo, I. Castagliuolo, P. Brun, F. Tonus, A. Ferrarese, A. Guiotto, A. Chilin, Quinazoline-based multi-tyrosine kinase inhibitors: synthesis, modeling, antitumor and antiangiogenic properties, European Journal of Medicinal Chemistry 67 (2013) 373–383.
[9] F. Xu, L. Zhang, Y. Jia, X. Wang, X. Li, Q. Wen, Y. Zhang, W. Xu, Discovery of 4-amino-2-(thio)phenol derivatives as novel protein kinase and angiogenesis inhibitors for the treatment of cancer: synthesis and biological evaluation. Part II, European Journal of Medicinal Chemistry 69 (2013) 191–200.
[10] A. Bronckaers, F. Gago, J. Balzarini, S. Liekens, The dual role of thymidine phosphorylase in cancer development and chemotherapy, Medicinal Research Reviews 29 (2009) 903–953.
[11] I.V. Bijnsdorp, F. Capriotti, F.A.E. Kruyt, N. Losekoot, M. Fukushima, A.W. Griffioen, V.L. Thijssen, G.J. Peters, Thymidine phosphorylase in cancer cells stimulates human endothelial cell migration and invasion by the secretion of angiogenic factors, British Journal of Cancer 104 (2011) 1185–1192.
[12] G.J. Peters, I.V. Bijnsdorp, M. Fukushima, Thymidine phoshorylase as a target for antiangiogenesis treatment, Nucleic Acids Symposium Series 52 (2008) 629.

[13] S. Liekens, A. Bronckaers, M.J. Pérez-Pérez, J. Balzarini, Targeting platelet-derived endothelial cell growth factor/thymidine phosphorylase for cancer therapy, Biochemical Pharmacology 74 (2007) 1555–1567.
[14] M.J. Pérez-Pérez, E.M. Priego, A.I. Hernández, M.J. Camarasa, J. Balzarini, S. Liekens, Thymidine phosphorylase inhibitors: recent developments and potential therapeutic applications, Mini-Reviews in Medicinal Chemistry 5 (2005) 1113–1123.
[15] H. Bera, B.J. Tan, L. Sun, A.V. Dolzhenko, W.K. Chui, G.N. Chiu, A structure-activity relationship study of 1,2,4-triazolo[1,5-*a*][1,3,5]triazin-5,7-dione and its 5-thioxo analogues on anti-thymidine phosphorylase and associated anti-angiogenic activities, European Journal of Medicinal Chemistry 3 (2013) 325–334.
[16] L. Sun, H. Bera, W.K. Chui, Synthesis of pyrazolo[1,5-*a*][1,3,5]triazine derivatives as inhibitors of thymidine phosphorylase, European Journal of Medicinal Chemistry 65 (2013) 1–11.
[17] L. Sun, J. Li, H. Bera, A.V. Dolzhenko, G.N. Chiu, W.K. Chui, Fragment-based approach to the design of 5-chlorouracil-linked-pyrazolo[1,5-*a*][1,3,5]triazines as thymidine phosphorylase inhibitors, European Journal of Medicinal Chemistry 70 (2013) 400–410.
[18] M. Fukushima, N. Suzuki, T. Emura, S. Yano, H. Kazuno, Y. Tada, Y. Yamada, T. Asao, Structure and activity of specific inhibitors of thymidine phosphorylase to potentiate the function of antitumor 2'-deoxyribonucleosides, Biochemical Pharmacology 59 (2000) 1227–1236.
[19] J. Balzarini, A.E. Gamboa, R. Esnouf, S. Liekens, J. Neyts, E. De Clercq, M.J. Camarasa, M.J. Pérez-Pérez, 7-Deazaxanthine, a novel prototype inhibitor of thymidine phosphorylase, FEBS Letters 438 (1998) 91–95.
[20] T. Yoshino, N. Mizunuma, K. Yamazaki, T. Nishina, Y. Komatsu, H. Baba, A. Tsuji, K. Yamaguchi, K. Muro, N. Sugimoto, Y. Tsuji, T. Moriwaki, T. Esaki, C. Hamada, T. Tanase, A. Ohtsu, TAS-102 monotherapy for pretreated metastatic colorectal cancer: a double-blind, randomised, placebo-controlled phase 2 trial, Lancet Oncology 13 (2012) 993–1001.
[21] A.V. Dolzhenko, A.V. Dolzhenko, W.K. Chui, Pyrazolo[1,5-*a*][1,3,5]triazines (5-aza-9-deazapurines). Synthesis and biological activity, Heterocycles 75 (2008) 1575–1622.
[22] P.N. Craig, Interdependence between physical parameters and selection of substituent groups for correlation studies, Journal of Medicinal Chemistry 14 (1971) 680–684.
[23] J. Kobe, R.H. Springer, D.E. O'Brien, Pyrazolo(1,5-a)1,3,5-triazines pat. US 3846423, 1974.
[24] B. Koren, F. Kovac, A. Petric, B. Stanovnik, M. Tisler, Heterocycles. CXXXIII. Indazoles in organic synthesis. Formation of some fused heterocycles, Tetrahedron 32 (1976) 493–497.
[25] K.S. Gudmundsson, B.A. Johns, J. Weatherhead, Pyrazolopyrimidines and pyrazolotriazines with potent activity against herpesviruses, Bioorganic & Medicinal Chemistry Letters 19 (2009) 5689–5692.
[26] S. Kamila, B. Koh, E.R. Biehl, Microwave-assisted "green" synthesis of 2-alkyl/arylbenzothiazoles in one pot: a facile approach to anti-tumor drugs, Journal of Heterocyclic Chemistry 43 (2006) 1609–1612.
[27] I. Kim, J.H. Song, C.M. Park, J.W. Jeong, H.R. Kim, J.R. Ha, Z. No, Y.L. Hyun, Y.S. Cho, N. Sook Kang, D.J. Jeon, Design, synthesis, and evaluation of 2-aryl-7-(3',4'-dialkoxyphenyl)-pyrazolo[1,5-*a*]pyrimidines as novel PDE-4 inhibitors, Bioorganic & Medicinal Chemistry Letters 20 (2010) 922–926.
[28] F. Tayyari, D.E. Wood, P.E. Fanwick, R.E. Sammelson, Monosubstituted malononitriles: efficient one-pot reductive alkylations of malononitrile with aromatic aldehydes, Synthesis (2008) 279–285.
[29] T.A. Krenitsky, S.R.M. Bushby, U.S. Patent, 4, 178, 212, 1–8, Burroughs Welcome Co., Research Triangle Park, NC, 1979.
[30] G. Navarrete-Vazquez, P. Paoli, I. Leon-Rivera, R. Villalobos-Molina, J.L. Medina-Franco, R. Ortiz-Andrade, S. Estrada-Soto, G. Camici, D. Diaz-Coutino, I. Gallardo-Ortiz, K. Martinez-Mayorga, H. Moreno-Diaz, Synthesis, *in vitro* and computational studies of protein tyrosine phosphatase 1B inhibition of a small library of 2-arylsulfonylaminobenzothiazoles with anti-hyperglycemic activity, Bioorganic Medicinal Chemistry 17 (2009) 3332–3341.
[31] J. Balzarini, B. Degrève, A. Esteban-Gamboa, R. Esnouf, E. De Clercq, Y. Engelborghs, M.J. Camarasa, M.J. Pérez-Pérez, Kinetic analysis of novel multisubstrate analogue inhibitors of thymidine phosphorylase, FEBS Letters 483 (2000) 181–185.
[32] Y. Sullu, G.G. Demirag, A. Yildirim, F. Karagoz, B. Kandemir, Matrix metalloproteinase-2 (MMP-2) and MMP-9 expression in invasive ductal carcinoma of the breast, Pathology Research and Practice 207 (2011) 747–753.
[33] A. Hoeben, B. Landuyt, M.S. Highley, H. Wildiers, A.T. Van Oosterom, E.A. De Bruijn, Vascular endothelial growth factor and angiogenesis, Pharmacological Reviews 56 (2004) 549–580.
[34] G. Finkenzeller, A. Sparacio, A. Technau, D. Marmè, G. Siemeister, Sp1 recognition sites in the proximal promoter of the human vascular endothelial growth factor gene are essential for platelet-derived growth factor-induced gene expression, Oncogene 15 (1997) 669–676.
[35] L.A. Liotta, W.G. Stetler-Stevenson, Metalloproteinases and cancer invasion, Seminars in Cancer Biology 1 (1990) 99–106.
[36] M.C. Alley, D.A. Scudiero, A. Monks, M.L.M.J. Hursey Czerwinski, D.L. Fine, B.J. Abbott, J.G. Mayo, R.H. Shoemaker, M.R. Boyd, Feasibility of drug screening with panels of human tumor cell lines using a microculture tetrazolium assay, Cancer Research 48 (1988) 589–601.
[37] E. Mitsiki, A.C. Papageorgiou, S. Iyer, N. Thiyagarajan, S.H. Prior, D. Sleep, C. Finnis, K.R. Acharya, Structures of native human thymidine phosphorylase and in complex with 5-iodouracil, Biochemical and Biophysical Research 386 (2009) 666–670.
[38] P.K. Ojha, K. Roy, First report on exploring structural requirements of alpha and beta thymidine analogs for PfTMPK inhibitory activity using in silico studies, Biosystems 113 (2013) 177–195.
[39] R.A. Norman, S.T. Barry, M. Bate, J. Breed, J.G. Colls, R.J. Ernill, R.W.A. Luke, C.A. Minshull, M.S.B. McAlister, E.J. McCall, H.H.J. McMiken, D.S. Paterson, D. Timms, J.A. Tucker, R.A. Pauptit, Crystal structure of human thymidine phosphorylase in complex with a small molecule inhibitor, Structure 12 (2004) 75–84.